Finite Element Analysis of Cage Subsidence in Cervical Interbody Fusion

Ming-Fu Chiang[1,2] Jui-Min Teng[3] Chang-Hung Huang[3, 4] Cheng-Kung Cheng[3,4,5,*]

Chen-Sheng Chen[5] Ting-Kuo Chang[3, 6] Shi-Hui Chao[4]

[1]Department of Neurosurgery, Mackay Memorial Hospital, Taipei, Taiwan, 104 ROC
[2]Mackay Medicine, Nursing and Management College, Taipei, Taiwan 112 ROC
[3]Institute of Biomedical Engineering, National Yang-Ming University, Taipei, Taiwan, 112 ROC
[4]Joint Prosthesis Technology Research Center, National Yang-Ming University, Taipei, Taiwan, 112 ROC
[5]Institute of Rehabilitation Science and Technology, National Yang-Ming University, Taipei, Taiwan, 112 ROC
[6]Department of Orthopaedic Surgery, Mackay Memorial Hospital, Taipei, Taiwan, 104 ROC

Received 2 Nov 2004; Accepted 15 Dec 2004

Abstract

Cages were used frequently in cervical spine interbody fusion to get better fusion rate. However, the fusion cage would subside in adjacent vertebral body. Three dimensional cervical spine model of C4-C6 was constructed referring to our previous model procedure (FEM). The suitable location of fusion cage had discussed with experienced surgeons and then cervical interbody fusions were simulated by finite element analysis. Factors caused subsidence, including (1) different moment loadings; (2) cage geometry; (3) cage material and (4) bone mineral density were also simulated. The results showed that extension of cervical spine caused remarkable subsidence than average value about 31.8%, next were flexion (13.8%), lateral bending (10.8%), and torsion. Cylindrical shape cage (BAK) appeared a higher risk of subsidence (6.6%) and von-Mises stresses (10.1%) than ring-liked shape cage (SOLIS). Comparing the cage material, the BAK cage made the settlement higher to 11% and the stress increased to 33.8%. The subsidence increased to 21.2% related to intact model in both cages while osteopenia of bony density were simulated. In conclusion, in the ROMs, extension motion caused remarkable subsidence after cages fusion. The geometry of the cage should keep from the cylinder or sharp angle, and the composed material of the cage is suggested to be closed to bone density for avoiding stress shielding. Patients with osteopenia will increase subsidence in cage interbody fusion

Keywords: Cage, Cervical interbody fusion, Finite element analysis, Range of motion (ROM), Subsidence

Introduction

Degenerative diseases of cervical discs are commonly treated with anterior cervical discectomy and fusion (ACDF). During surgery, the physiological disc height has to be restored to prevent compression of the nerve roots and the spinal cord [1]. For this purpose, intervertebral spacers such as interbody fusion cages, bone cement, bone graft, or biodegradable polymers or ceramics are implanted [2]. These implants should not only restore the physiological disc height but also maintain it, thereby preventing graft collapse or subsidence into the adjacent vertebral [3-7]. Cages filled with cancellous bone would reduce donor site pain, a common problem associated with harvesting of structural iliac grafts. However, metallic cages have the potential to corrode over extended periods. They also can cause bone resorption, and inflammation caused by micromotion or stress shielding as well as loosening [4-7]. Cervical interbody fusion cages may subside into the adjacent vertebrae with collapse of the intervertebral space and kyphotic deformation of the affected segment. Complications such as cage dislocation or nonunion with instability also have been reported [5-7].

Wilke et al [8, 9] and Kettler et al [10] used three kinds of cages and bone cement to investigate the effect of simulated postoperative neck movements on the subsidence and analyze different kinds of cage designs and materials affect the subsidence and stability. The results showed that the subsidence of carbon fiber cage was only half value of that metallic cage. Otherwise, the carbon cage had better stability. Furderer et al [11] used forty-five bovine vertebral bodies to compare the subsidence of differently designed cervical interbody fusion devices under defined conditions. They showed that abrasion of

* Corresponding author: Cheng-Kung Cheng.
Tel: +886-2-28267020; Fax: +886-2-28202519
E-mail: ckcheng@ortho.ym.edu.tw

Table 1: The material properties specified in the finite element models

Component	E (MPa)	γ	A (mm^2)
Vertebra			
Cortical bone	12000	0.30	-
Cancellous bone	100	0.20	-
Posterior elements	3500	0.29	-
Disc			
Nucleus	1.0	0.49	-
Ground substance	3.4	0.40	
Fiber	450	0.30	0.76
Endplate	500	0.40	
Ligament			
Anterior longitudinal ligament	10	-	11.10
Posterior longitudinal ligament	20	-	11.30
Ligamentum flavum	50	-	46.00
Interspinous ligament	3	-	13.00
Supraspinous ligament	3	-	5.00
Facet joint			
Facet synovial fluid	3	0.49	-
Facet synovial membrane	12	0.40	-
Cage			
Titanium alloy cage	113×10^3	0.3	
PEEK polymer cage	1.3×10^3	0.2	

NOTE: E, Young's modulus (MPa); γ, Poisson's ratio; A, Section-area (mm^2)

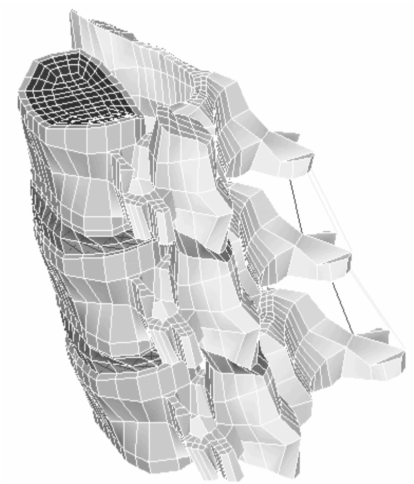

Figure 1.The FEM of the three-dimensional cervical spine (C4-C6) included ligaments, disc, vertebral body, and posterior element.

the end plate resulted in an increased subsidence and the subsidence was higher in the cylindrical cage when the end plate was taken off.

In 2002, Kandziora et al. [12-14] performed an *in vitro* biomechanical study of cervical spine interbody fusion cages by using a sheep model. On the contrary, the biomechanical results indicated that design variations in screw and cylinder design groups were of little importance. Besides, the result showed that *in vitro* study couldn't reflect the real situation of *in vivo* fusion due to the stiffness of individually cervical spine was significantly different. In order to elucidate the biomechanics of cervical cage subsidence, this study was aimed to use finite element method to analyze factors affected the subsidence, including (1) different moment loadings; (2) cage geometry; (3) cage material; and (4) bone mineral density.

Materials and methods

Intact cervical spine model

To identify the relationships between those factors and subsidence, the present study created a three-dimensional finite element model (FEM) of the cervical spine, which included three vertebral body and two discs from the C4 to C6 vertebral body. The commercially available finite element program, ANSYS 7.0 (Swanson Analysis System Inc., Houston, TX) was used to model the spinal segments [15-19]. Computed tomographic scanning images of the normal cervical spine of a 48-year-old female subject were obtained using transverse slices at every 3-mm interval. Each CT slice was acquired from the coronal plane and enlarged in order to identify the different regions of the tissues. At the same time, its position in a global coordinate system was calculated from roentgenograph, as well as its sagittal inclination due to lordosis. The coordinates of the nodal point were digitized in terms of the X- and Y- coordinates in each CT slice. The X-axis was defined as the mediolateral direction of the vertebral body and the Y-axis as the anteroposterior direction of the vertebral body. The orientation of each articular facet was modified to ensure the geometric congruence between adjacent articular facets which were connected with intervertebral discs and the ligaments. These ligaments were defined using lines to join their approximate attachment points on adjacent vertebrae. The edge of the spinal disc was obtained from the enhanced CT images. But the geometry of the disc nucleus was difficult to distinguish from the CT image and the study referred to Panagiotacopulos et al.'s study [20]. The 30–50 % of the total disc area in cross-section was defined as the disc nucleus of the FEM, and the rest of the region was assumed as the disc annulus of the FEM. The FEM of the ligamentous cervical spine consisted of vertebrae, intervertebral discs, superior and inferior facet articulating surfaces, and a number of ligaments: supraspinous, interspinous, ligamentum flavum, posterior longitudinal, anterior longitudinal. The material properties were adopted from related literature [21-26] as Table 1 shows. The cable elements were used to simulate ligaments and annulus fiber of disc, which were active only in tension. The rest of the portions assigned as the solid elements included the vertebral body, posterior element, the disc annulus, and the disc nucleus. The whole model of the cervical spine contained 4796 elements and 6998 nodes. The typical view of the reconstructed three-dimensional model is shown as Figure 1.

Model validation

Because of few studies carried out *in vitro* for moments (flexion, extension, lateral bending, and torsion), the C4–C6 model with C4 removed formed the C5–C6 motion segment for validation against *in vitro* experimental results and analytical models. In these series of analyses, the C5–C6 model

Table 2: The present range of motion (ROM) data compared with the experimental and previous finite element data

Degree(°)	Moroney et al. (1988)	Ng et al. (2003)	Present (2004)
Flexion	5.55 (1.84)	4.83	6.32
Extension	3.52 (1.94)	3.95	4.16
Bending	4.71 (2.99)	1.58	5.24
Torsion	1.85 (0.67)	2.43	2.21

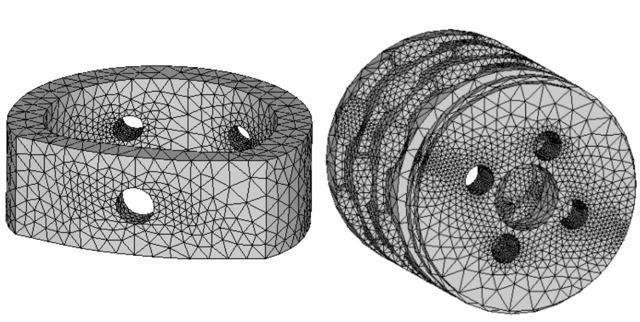

(a) (b)

Figure 2. The finite element model of cervical fusion cages, (a) SOLIS; (b) BAK.

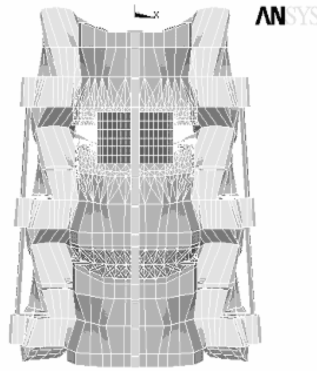

(a)

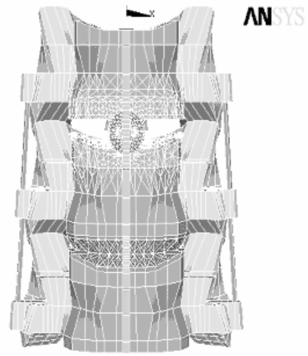

(b)

Figure 3. The interbody fusion cage model was simulated at C4-5 level, (a) SOLIS; (b) BAK.

was fixed in all directions at the inferior surface of C6. An axial compressive load of 73.6 N was applied, and eventually a distributed pure moment of 1.8 N-m in flexion or extension was applied incrementally in nine equal steps over the top surface of the C5 vertebra to simulate the experimental loads used by Moroney et al. [28, 29] For the C5–C6 model, with the applied moment at C5, two nodal points on the superior C5 body were selected to determine the rotation of the C5 vertebra with respect to C6 in the plane of moment application. The rotational motion obtained was compared with the results found in the literature. The two-level model predicted primary motions very close to those of the mean experimental [28, 29] and finite element model simulated data [30, 31] in flexion, extension, and axial torsion (Table 2). The four kinds of moment loads fell within 1 standard deviation of the experimental mean values. The current model predicted the primary motions in close agreement with the experimental values. All the analyses were performed using ANSYS 7.0 with nonlinear static structural contact, solution control, and time stepping options.

Cage models

Two kinds of commercial cages were reconstructed with the software of Pro/E 2001 (Parametric Technology Corporation) and then transferring the model into ANSYS interface. Both different shape of commercial cages (Figure 2) were simulated in the study including: cylindrical shape (BAK, Sulzer Spine-Tech, Minneapolis, USA) and ring-liked shape (SOLIS, Stryker Instruments, Kalamazoo, USA). The composed of material of BAK is titanium alloy and the other was proprietary composites such as carbon-fiber reinforced PEEK (polyetheretherketon).

Interbody fusion cage model

The intact FEM described above was modified to simulate the anterior cervical discectomy and fusion (ACDF). To mimic the surgery, the disc was totally removed and then replaced by the interbody fusion cage [27]. The assumption of the study was that the patients have not yet gained totally solid fusion, so the contact surface between the bone and cage within the model was determined by assuming that the interbody bone cage would be able to transmit loads in compression, but not as well as in extension. So the surface was used the contact element (contact174) to simulate the primary stage of fusion. According to the purposes of this study it was necessary to build two fused models as follow: BAK at C4-5, SOLIS at C4-5, as shown in Figure 3.

Boundary and loading condition

In the three-level FEM, the degrees of freedom of inferior surfaces of the inferiormost vertebral body were completely fixed in all directions. The kinematics data of the present modified C4-6 FEM model were compared with the *in vitro* experiment and other FEM model under the same loading conditions which included flexion, extension, torsion, and lateral bending for the validation [28-31]. The two-level model was subjected to a moment of 1.8 Nm with a preload of 73.6N at the C5 vertebra similar to those used by Morony et al [28, 29]. The maximum load was achieved in nine load steps in the FEM. Because of the stress accumulation caused by different loads, it was necessary to consider the overall stress variation in the estimated results of the FEM. Consequently, the subsidence results were calculated with the maximum

Table 3: Subsidence in motion loadings of the two fused models. (Unit: mm)

Model	Subsidence of SOLIS at C4-5			Subsidence of BAK at C4-5		
Material E*	PEEK 100MPa	PEEK 70MPa	Ti-alloy 100MPa	Ti-alloy 100MPa	Ti-alloy 70MPa	PEEK 100MPa
Flexion	1.22	1.59	1.51	1.59	1.79	1.51
Extension	1.45	1.91	1.88	1.84	2.35	1.75
Bending	1.14	1.44	1.36	1.43	1.93	1.36
Torsion	0.36	0.42	0.41	0.77	0.80	0.61

NOTE: E*:Young's modulus of cancellous bone

Table 4: The von-Mises stress of the maximum subsidence on the contact surface in different motion loadings of the two fused models (Unit: MPa)

Model	von-Mises stress of SOLIS at C4-5			von-Mises stress of BAK at C4-5		
Material E*	PEEK 100MPa	PEEK 70MPa	Ti-alloy 100MPa	Ti-alloy 100MPa	Ti-alloy 70MPa	PEEK 100MPa
Flexion	6.66	6.80	9.89	9.12	9.51	7.13
Extension	8.09	8.28	12.63	11.26	11.33	8.50
Bending	9.14	9.23	12.79	11.55	11.78	8.84
Torsion	4.88	5.36	6.92	7.33	7.36	5.52

NOTE: E*:Young's modulus of cancellous bone

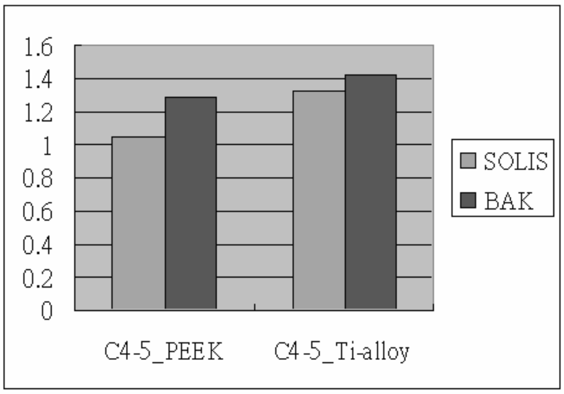

Figure 4. Comparisons of the subsidence by different cage shapes (unit: mm).

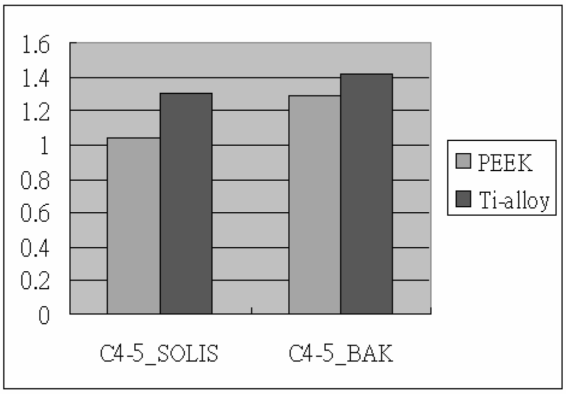

Figure 5.Comparison of the subsidence by different cage materials (unit: mm).

settlement of the cage, and the stress results were expressed in terms of maximum von-Mises stresses.

Factors design

In this study, four factors were analyzed. First of all, the different moment loadings included flexion, extension, torsion, and lateral bending. The fused models were loaded separately by the four moments to identify which one influenced the cage settlement strongly. Secondly, there were two kinds of cage geometries selected in this study, and they were cylindrical BAK and ring-like SOLIS. The circumstance of the fused model was controlled similarity, and manifested the effect of geometry. Furthermore, the cage materials were discussed in the study. The titanium alloy and PEEK polymer were compared with each other in the same cage shape [32]. Besides, the bone mineral density (BMD) was considered to be the crucial point to affect subsidence. So it was workable to change the Young's modulus of cancellous bone to imitate the BMD of osteopenic patient. Homminga et al [33] brought out the equation between Young's modulus and BMD. The equation was $E=5.124\times\rho^{1.7}$, E represented Young's modulus of cancellous bone (GPa), and ρ was the bone mineral density (g/cm^3). Furthermore, their study declared that the BMD of regular people was higher than 0.1 g/cm^3, and the BMD of osteopenic patient was lower than 0.08 g/cm^3. So, in this study assumed that the normal BMD was 0.1 g/cm^3 and the BMD of osteopenia was 0.08g/cm^3, the corresponding Young's modulus separately were 100 MPa and 70 MPa.

Results

Subsidence in different moment loadings

Putting the subsidence of the two fusion models data into consideration, the tendency exists under different moment loadings as follow: no matter where cage was put into or what shape it was, the extension caused the maximum settlement higher than the mean subsidence of overall data to 31.8%. Next were flexion and bending (higher than mean value amount to 13.8% and 10.8% respectively), and the minimum settlement

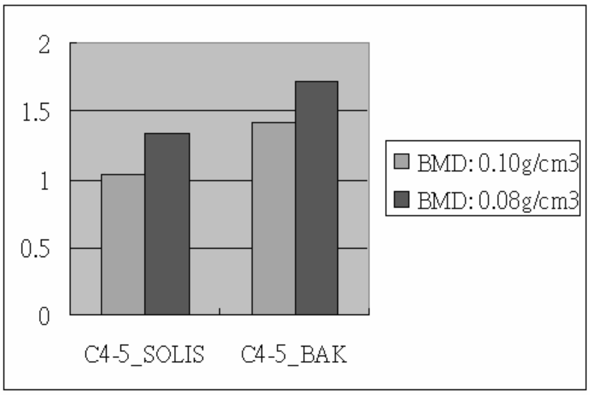

Figure 6. Comparison of the subsidence by different bone mineral density (unit: mm).

caused by torsion (lower than average value amount to 56.5%) (Table 3). In the aspect of the von-Mises stress of the maximum subsidence on the contact surface, the maximum stress caused by bending (higher than average to 18.9%), next was extension (higher than average to 17.2%), and torsion (lower than average 33.6%) (Table 4).

Subsidence in different cage geometries

Two kinds of cage geometries frequently used in clinical which were chosen to simulate in this study. They were cylindrical shape (BAK) and ring-liked shape (SOLIS). The material property was set the same to compare the subsidence caused by different shapes. The results showed that no matter what material cage was or where it was put into, the BAK shape caused higher subsidence than SOLIS to 6.6% (Figure 4). The contact surface stresses had the same trend. The BAK shape caused the stresses average higher than SOLIS to 36.9%.

Subsidence in different cage materials

Many clinical follow-up studies showed the complications like inflammation, corrode, subsidence, stress shielding, and metallosis etc. [5-7, 34] were found in the cage which were made of stainless steel. Therefore, the material was gradually improved as the present stuffs. In this study, choosing two kinds of common material compared their properties effect of cage settlement. The results showed that no matter what cage shape was or where it was put into, the titanium-alloy caused more subsidence than PEEK average to 11% (Figure 5), and the contact surface stresses also showed the same trend that the titanium-alloy got rise to higher stress than PEEK average to 33.8%.

Subsidence related to bone mineral density (BMD)

Many previous studies discussed the issue about the relationship between bone mineral density and subsidence, but it is still controversial [8-14]. In this study, the normal BMD was assumed to be 0.10 g/cm^3 and was reduced 0.02 g/cm^3 to simulate osteopenia. The results calculated from finite element method showed that reducing the BMD increased the subsidence to 21.2% in proportion to normal (Figure 6). Especially, the increment is higher in SOLIS (25.3%) than the BAK (17.0%).

Discussion

According to Wilke et al.'s study [8, 9], 24 human cervical spine specimens were tested after stabilization with either a WING, BAK/C, AcroMed I/F cage and bone cement. Then, 700 pure-moment loading cycles were applied in the directions (lateral bending, flexion–extension, and axial rotation alone or in combination with each other) to simulate the patient's neck movements during the first few postoperative days. Measurements of the subsidence depth (loss of total height) in combination with flexibility tests were performed before cyclic loading and after. The results showed that cyclic loading caused subsidence in all four groups, most distinct with BAK/C-cages (1.63 mm) followed by the new WING (0.90mm) and the AcroMed (0.82 mm) cages. In this study, after four simulated moment loadings, the subsidence of BAK was 1.34 mm and SOLIS was 0.96 mm, it was obviously higher than experimental data. It is well known that finite element models cannot exactly predict the results which compared with the result obtained from *in vitro* study. The reason is that the dimension of the model was not the same with *in vitro* specimen and also difficultly imitated the cyclic loadings by finite element analysis. Furthermore, the simulated material properties of various components of the model were referred as related literatures, and assumed the properties as homogenous and isotropic. It is different from the cadaveric specimens.

Different moment loadings

The reason why extension motion caused the maximum subsidence was speculated that the cage was directly put on the bone and eliminated the endplate, so the anterior and posterior of the cage was above the cortical bone and cancellous bone. Consequently, when extension leaded to higher stress at the posterior part of cage and immediately raised subsidence on the adjacent cancellous bone. An unknown situation still existed, why the lateral bending motion could cause maximum contact stress, but not leaded to the highest settlement. The explanation might be that bending moment caused the axial compressive stress while compare than other motions. Additionally, according to the von-Mises stress equation, the three axial stresses played the same important roles in influencing the result. It could be explained that the other two directional stresses in lateral bending were higher than other motions, therefore the cage settlement was not greater than others.

Cage geometry

As the results of Wilke et al.[8, 9], there were no significant difference found among their simulated cage designs. Similarly, the two kinds of cage types analyzed in this study showed an unapparent subsidence (BAK higher than SOLIS to 6.6%). but there was significant divergence on the contact stress between both designs (BAK higher than SOLIS 36.9%). The cylindrical shape caused higher comparatively concentrated stress than that of ring-like shape. Besides, the BAK is designed with screw thread which could cause concentrating stress nearby the edge of this cage. It's suggested to keep from this kind of shape to reduce contact stress.

Cage material

Presently, there were many kinds of materials used in cages, including stainless steel, titanium alloy, biodegradable polymer, ceramics, etc. Many experts tried so hard to work out the most suitable material for fusion cage, but there were still complications existed postoperatively. In this study, we tried to identify which one could cause less subsidence. The results showed that the PEEK produced the less subsidence and lower contact stress significantly. The explanation to the consequence was that the difference between the Young's modulus of the two materials. The young's modulus of Ti-alloy (E=113GPa) was much higher than that of cancellous bone (100MPa), but the PEEK (E=1.3GPa) was closer to the bone's modulus when compared with Ti-alloy[32]. The huge Young's modulus difference could not only cause the higher subsidence but also cause the stress shielding at the interface.

Bone mineral density

The bone mineral density (BMD) is also an important factor leading to the risk of cage subsidence. According to Wilke et al.'s studies [8, 9], only a moderate correlation between bone mineral density and subsidence depth could be found in the BAK/C group (r^2=0.495). It didn't seem to have enough evidence to give a clear definition between the BMD and subsidence. So we tried to use finite element method to predict the relationship. As the results showed, when the BMD decreased 0.02 g/cm^3, the subsidence depth increased 21.2%. There is a high correlation between bone density and cage subsidence. There was an interesting trend that when the BMD decreased, the SOLIS produced more distinct settlement than that of BAK. The tendency showed an uncertain answer: the higher contact area of cage was designed, the more subsidence happened on the lower BMD. This result still needs further studies to confirm.

Conclusion

Simulations of the postoperative neck movements caused subsidence in two kinds of cervical spine interbody fusion cages were reported. The ring-liked shape cage (SOLIS) has a better resistance against subsidence than the cylindrical shape cage (BAK). In general, with a large contact area at the implant–bone interface is able to reduce the subsidence risk. The effect of the BMD on the subsidence risk was clearly presented. Especially, the vertebrae with a decreased BMD showed to increase the subsidence risk of cage which was in direct contact to the cancellous bone. Besides, comparison of cage geometries showed that the cylindrical design could not offer the enough resistance to reduce subsidence. In the aspect of cage material, the PEEK showed better ability to resist subsidence than Ti-alloy.

Acknowledgements

This study was supported by a Grant (MMH-9238) from the Department of Medical Research, Mackay Memorial Hospital, Taipei, Taiwan.

Reference

[1] G. Matge, "Cervical cage fusion with 5 different implants: 250 cases", *Acta. Neurochir.,* 144:539-549, 2002.

[2] K. Totoribe, M. Matsumoto, V.K Goel, S.J. Yang, N. Tajima, Y. Shikinami, "Comparative biomechanical analysis of a cervical cage made of an unsintered hydroxyapatite particle and poly-L-lactide composite in a cadaver model", *Spine*, 28:1010-1015, 2003.

[3] G.W. Bagby, "Arthrodesis by the distraction-compression method using a stainless steel implant", *Orthopedics*, 11:931-934, 1988.

[4] R.J. Friedman, J. Black, J.O. Galante, "Current concepts in orthopaedic biomaterials and implant fixation", *J. Bone Joint Surg.,* 75(A): 1085-1109, 1993.

[5] S. Takahashi, J. Delecrin, N. Passuti, "Intraspinal metallosis causing delayed neurologic symptoms after spinal instrumentation surgery", *Spine* 26:1495-1498, 2001.

[6] V.K. Goel, Y.E. Kim, T.H. Lim, "An analytical investigation of the mechanics of spinal instrumentation", *Spine,* 13: 1003-1011, 1988.

[7] R.S. Hatch, P.F. Sturm, C.C. Wellborn,"Late complication after single-rod instrumentation", *Spine,* 23: 1503-1505, 1998.

[8] H.J. Wilke, A. Kettler, L, Claes, "Primary stabilizing effect of interbody fusion devices for the cervical spine: an in vitro comparison between three different cage types and bone cement", *Europ. Spine J.* 9: 410-416, 2000.

[9] H.J. Wilke, A. Kettler, C. Goetz, L. Claes, "Subsidence resulting from simulated postoperative neck movements: an in vitro investigation with a new cervical fusion cage", *Spine* 25: 2762-2770, 2000.

[10] A Kettler, HJ Wilke, L Claes, "Effects of neck movements on stability and subsidence in cervical interbody fusion: an in vitro study", *J. Neurosurg.,* 94: 97-107, 2001.

[11] S. Furderer, F. Schollhuber, J.D. Rompe, P. Eysel,"Effect of design and implantation technique on risk of progressive sintering of various cervical vertebrae cages", *Orthopedics,* 31: 466-471, 2002.

[12] F. Kandziora, R. Pflugmacher, J. Schafer, C. Born, G. Duda, N.P. Haas, T. Mittlmeier, "Biomechanical comparison of cervical spine interbody fusion cages", *Spine* 26: 1850-1857, 2001.

[13] F. Kandziora, R. Pflugmacher, M. Scholz, J. Schafer, G. Schollmeier, K.J. Schnake, H.Bail, H, Duda, H.P. Haas, "Experimental fusion of the sheep cervical spine. Part I: Effect of cage design on interbody fusion", *Chirurg.,* 73: 909-917, 2002.

[14] F. Kandziora, G. Schollmeier, M. Scholz, J. Schaefer, A. Scholz, G. Schmidmaier, R. Schroder, H. Bail, G. Duda, T. Mittlmeier, N.P. Haas, "Influence of cage design on interbody fusion in a sheep cervical spine model", *J. Neurosurg.,* 96:321-332, 2002

[15] C.S. Chen, C.K. Cheng, C.L. Liu, W.H. Lo, "Stress analysis of the disc adjacent to interbody fusion in lumbar spine". *Med. Eng. Phys.,* 23: 483-491, 2001

[16] C.K. Cheng, C.S. Chen, C.L. Liu, "Biomechanical analysis of the lumbar spine with anterior interbody fusion on the different locations of the bone grafts", *Biomed. Mater. Eng.,* 12:367-374, 2002

[17] C.S. Chen, C.K. Cheng, C.L. Liu, "A biomechanical comparison of posterolateral fusion and posterior fusion in the lumbar spine". *J. Spinal Disord. Tech.,* 15:53-63, 2002

[18] C.S. Chen, C.K. Feng, M.J. Tzeng, C.L. Liu, W.J. Chen, C.K. Cheng, "Biomechanical analysis of the disc adjacent to posterolateral fusion with laminectomy in lumbar spine". *J. Spinal Disord. Tech.,* 2004 (In press)

[19] C.K. Cheng, W.J. Chen, C.S. Chen, S.C. Chueh, C.C. Wang, "Failure analysis of pedicle screw breakage on spinal instrumentation". *Med. En.g Phys.,* 2004 (Accepted)

[20] N.D. Panagiotacopulos, M.H. Pope, M.H. Krag, R. Bloch, "A mechanical model for the human intervertebral disc". *J. Biomech.*

20(9): 839-50, 1987

[21] J.D. Clausen, V.K. Goel, V.C. Traynelis, J. Scifert, ”Uncinate processes and Luschka joints influence the biomechanics of the cervical spine: quantification using a finite element model of the C5-C6 segment”, *J. Orthop. Res.,* 15: 342-347, 1997

[22] S. Kumaresan, N. Yoganandan, F.A. Pintar, “Finite element analysis of the cervical spine: a material property sensitivity study”, *Clin. Biomech.,* 14: 41-53, 1999

[23] S. Kumaresan, N. Yoganandan, F.A. Pintar, D.J. Maiman, S. Kuppa, “Biomechanical study of pediatric human cervical spine: a finite element approach”, *J. Biomech. Eng.,* 122: 60-71, 2000.

[24] R.N. Natarajan, B.H. Chen, H.S. An, G.B. Andersson, “Anterior cervical fusion: a finite element model study on motion segment stability including the effect of osteoporosis”, *Spine,* 25: 955-961, 2000.

[25] T.R. Pitzen, D. Matthis, D.D. Barbier, W.I. Steudel, “Initial stability of cervical spine fixation: predictive value of a finite element model” *J. Neurosurg.* 97: 128-134, 2002.

[26] V.K. Goel, J.D. Clausen, “Prediction of load sharing among spinal components of a C5-C6 motion segment using the finite element approach”, *Spine* 23: 684-691, 1998.

[27] D.Y. Cho, W.R. Liau, W.Y. Lee, J.T. Liu, C.L. Chiu, P.C. Sheu, ”Preliminary experience using a polyetheretherketone (PEEK) cage in the treatment of cervical disc disease”, *Neurosurgery,* 51: 1343-1349, 2002.

[28] Moroney SP, Schultz AB, Miller JA: Analysis and measurement of neck loads. J *Orthop. Res.,* 6:713-720, 1988

[29] S.P. Moroney, A.B. Schultz, J.A. Miller, G.B. Andersson, “Load-displacement properties of lower cervical spine motion segments”, *J.Biomech.,* 21: 769-779, 1988.

[30] H.W. Ng, E.C. Teo, “Nonlinear finite-element analysis of the lower cervical spine (C4-C6) under axial loading”, *J. Spinal Disord. Tech.,* 14: 201-210, 2001.

[31] H.W. Ng, E.C. Teo, K.K. Lee, T.X. Qiu, “Finite element analysis of cervical spinal instability under physiologic loading”. *J. Spinal Disord. Tech.,* 16: 55-65, 2003.

[32] C. Adam, M. Pearcy, P. McCombe, “Stress analysis of interbody fusion:finite element modelling of intervertebral implant and vertebral body. *Clin. Biomech.,* 18(4): 265-72, 2003.

[33] J. Homminga, H. Weinans, W. Gowin, D. Felsenberg, R. Huiskes,” Osteoporosis changes the amount of vertebral trabecular bone at risk of fracture but not the vertebral load distribution”, *Spine* 15(26): 1555-1561, 2001.

[34] U. Agrillo, L. Mastronardi, F. Puzzilli, “Anterior cervical fusion with carbon fiber cage containing coralline hydroxyapatite: preliminary observations in 45 consecutive cases of soft-disc herniation”, *J. Neurosurg.* 96: 273-276, 2002.